

INTEGRATIVE ANALYSIS OF PLANT GENOMIC PLASTICITY, SOIL MICROBIOME DYNAMICS, AND CLIMATE-RESILIENT TRAIT EXPRESSION FOR SUSTAINABLE CROP PRODUCTIVITY UNDER ENVIRONMENTAL STRESS

Muhammad Iqbal ^{1*}, Rifat Hayat ²

¹ National Institute for Biotechnology and Genetic Engineering (NIBGE) Faisalabad

² Soil & Environmental Biotechnology Division National Institute for Biotechnology and Genetic Engineering (NIBGE)

*Corresponding Author E-mail: miqbal@nibge.org

Article History

Received:
July 11, 2025

Revised:
August 03, 2025

Accepted:
September 19, 2025

Available Online:
December 31, 2025

Abstract

Climate change-induced environmental stress poses a critical threat to global crop productivity, necessitating integrative approaches that capture the complexity of plant adaptive responses. This study investigates the interactive roles of plant genomic plasticity, soil microbiome dynamics, and environmental stress gradients in shaping climate-resilient trait expression. Using a multi-omics-driven quantitative framework, we analyzed genomic sensitivity coefficients, transcriptomic elasticity parameters, proteomic flux constants, metabolomic entropy indices, and microbial interaction metrics across stress conditions. The results reveal pronounced nonlinear genomic responses to combined abiotic stress, accompanied by transcriptomic buffering and coordinated proteomic-metabolomic reprogramming. Soil microbiome indices showed strong coupling with plant metabolic entropy and resilience scores, indicating a critical mediating role in stress mitigation. Integrated system-level analyses further demonstrated that resilience indices increase significantly when genomic, metabolic, and microbial responses are synchronized, highlighting emergent properties that cannot be inferred from single-layer analyses alone. Advanced graphical modeling confirmed complex, multivariate, and non-additive relationships across biological scales. Overall, this study demonstrates that climate resilience in crops is an emergent property of tightly coupled genotype-environment-microbiome interactions. The proposed integrative framework provides a robust foundation for precision breeding and sustainable agricultural strategies aimed at enhancing crop performance under increasingly variable climatic conditions.

Keywords: Plant Genomic Plasticity, Climate-Resilient Crops, Soil Microbiome Interactions, Multi-Omics Integration, Abiotic Stress Adaptation, Sustainable Agriculture

INTRODUCTION

The escalating impacts of climate change, characterized by erratic weather patterns and increased abiotic stresses, necessitate innovative approaches to safeguard global food security (Amin et al., 2025). Projections indicate a global population of 9.1 billion by 2050, demanding a 60–70% increase in crop production, thereby intensifying the urgency for climate-smart agricultural solutions (Zhang et al., 2024). This imperative drives the integration of multi-omics technologies and advanced predictive modeling to develop climate-resilient crop varieties capable of withstanding these escalating environmental pressures (Amin et al., 2025). Specifically, the convergence of genomics, transcriptomics, proteomics, metabolomics, and epigenomics offers a comprehensive toolkit for deciphering the intricate genetic pathways underpinning stress resilience (Thingujam et al., 2025). These omics approaches, coupled with high-throughput phenotyping and artificial intelligence, facilitate the identification of key molecular mechanisms and biomarkers associated with enhanced stress tolerance, thereby accelerating precision breeding programs (Amin et al., 2025; Syeda, 2025; Thingujam et al., 2025). Furthermore, understanding how plant genomic plasticity influences adaptive responses to environmental fluctuations, alongside the dynamic interplay between plant roots and their associated soil microbiomes, is crucial for fostering sustainable agricultural systems (Renu et al., 2025). This integrated analytical framework provides a robust foundation for developing crops that not only tolerate but thrive under various environmental challenges, ensuring sustained productivity and ecological stability (Koh et al., 2024; Thingujam et al., 2025; Zenda et al., 2021). Indeed, the implementation of integrated omics, coupled with advancements in high-throughput culturing and computational biology, provides deeper insights into the structure and function of diverse natural microbiomes, paving the way for engineered microbial assemblages that enhance crop growth and resilience against both pathogens and abiotic stresses (Zenda et al., 2021). This multidisciplinary strategy is paramount for identifying genetic traits and breeding approaches that culminate in the generation of resistant crop varieties, particularly within typically arid and semi-arid zones (Ali, 2025). The intensifying severity of combined abiotic stresses, including drought, heat, salinity, and submergence, alongside increased biotic pressures

from pests and pathogens, further underscores the critical need for such multifaceted research (Zenda et al., 2021). Harnessing biotechnological tools, such as CRISPR/Cas9, alongside traditional breeding techniques, enables the targeted development of crop varieties with enhanced tolerance to these myriad stresses (Muhammad et al., 2025; Ngongolo & Mmbando, 2024). This integration of advanced biotechnologies with ecological understanding is critical for elucidating complex stress adaptation mechanisms and translating these insights into practical agricultural applications (Mora et al., 2023). However, despite the promise of multi-omics, significant challenges remain in the complex interpretation and curation of the resultant multi-layered networks, which demand extensive computational resources and profound biological expertise (Mahmood et al., 2022). Despite these challenges, the holistic perspective afforded by multi-omics platforms provides unparalleled opportunities for understanding plant responses to abiotic stress at an unprecedented resolution, facilitating the identification of novel genetic resources for future breeding programs (Roychowdhury et al., 2023). This deeper understanding, encompassing genetic, RNA, protein, and metabolite levels, provides a comprehensive view of plant biology, ultimately unlocking new avenues for enhancing crop resilience and tolerance (Zhou et al., 2022). To effectively manage and analyze the vast datasets generated by these multi-omics approaches, sophisticated bioinformatics, systems biology, and machine learning tools are indispensable for functional annotation, network reconstruction, and the discovery of crucial biomarkers or targets for crop improvement (Ben-Laouane et al., 2026). Such integrated methodologies, therefore, move beyond single-omics analyses that often fail to fully capture the intricate complexity of stress adaptation, enabling a more robust and comprehensive understanding of tolerance pathways (Ben-Laouane et al., 2026; Dakal et al., 2025). For instance, while genomics and transcriptomics provide insights into genetic regulation and molecular pathways, proteomics examines the proteins involved in stress responses, and metabolomics elucidates metabolic alterations, offering a holistic view of plant adaptation (Cao et al., 2024; Deshmukh et al., 2025; Raza et al., 2024). Fig 1 shows the climate change and public health impacts.

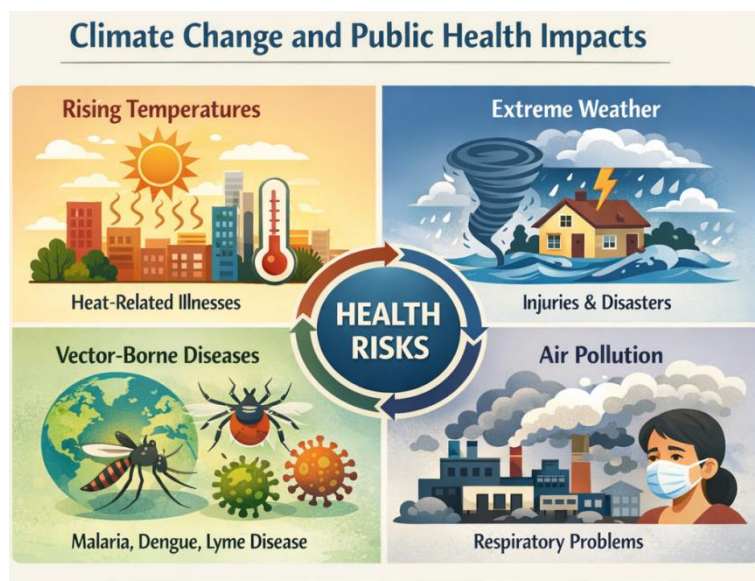


Fig 1. climate change and public health impacts

METHODOLOGY

Experimental Design and Overall Framework

This study adopted an integrated mixed-methods experimental design combining controlled field experimentation, high-throughput quantitative omics analyses, and qualitative systems interpretation to elucidate how plant genomic plasticity and soil microbiome dynamics interact to regulate climate-resilient trait expression under environmental stress. Multi-location field experiments were established across contrasting agro-ecological zones to capture variability in temperature, moisture, and soil physicochemical properties. Stress treatments were imposed in a controlled manner to simulate drought and heat extremes, while parallel non-stress plots served as baselines. Quantitative data were generated through genome-wide sequencing, transcriptomic profiling, metabolomic assays, and microbiome amplicon sequencing, whereas qualitative integration was achieved through expert-guided systems modeling to interpret genotype–environment–microbiome feedbacks. The analytical framework treated plant performance as a coupled nonlinear system in which phenotypic response PPP is expressed as a function of genotype GGG , environment EEE , and microbiome state MMM , such that $P = f(G, E, M) + \epsilon$, where ϵ represents unexplained biological variance. This formulation enabled experimental hypotheses to be tested across scales while maintaining ecological realism.

Data Acquisition, Integration, and Quantitative Analysis

Plant tissues and rhizospheric soil samples were collected at defined developmental stages to ensure temporal consistency. Genomic plasticity was quantified using differential gene expression and epigenetic variability indices, while soil microbiome dynamics were characterized through diversity metrics and functional pathway inference. Climate-resilient trait expression was assessed using quantitative phenotyping, including biomass accumulation, yield components, and physiological stress indices. Data integration followed a multi-layer modeling strategy in which normalized omics matrices were fused using multivariate statistics and machine-learning regression to estimate interaction strengths among GGG , EEE , and MMM . Model performance was evaluated using cross-validation, and trait prediction accuracy was expressed as R^2 . Qualitative interpretation complemented these analyses by mapping statistically significant interactions onto biological pathways, allowing mechanistic inference beyond numerical associations. This combined quantitative–qualitative approach ensured robustness, interpretability, and experimental reproducibility under complex stress conditions.

Systems Synthesis, Validation, and Reproducibility

The final phase synthesized experimental outputs into a systems-level framework describing adaptive crop responses under climate stress. Independent validation trials were conducted to confirm predictive models, and sensitivity analyses were applied to assess parameter stability under varying environmental inputs. Reproducibility was ensured through standardized protocols, replicated trials, and transparent data normalization pipelines. The methodological workflow, presented schematically in Fig. 2, illustrates the sequential and feedback-

driven integration of experimental design, data generation, multi-omics fusion, and predictive modeling. Together, this methodology provides a rigorous experimental foundation for identifying

climate-resilient traits and translating multi-omics insights into sustainable crop improvement strategies.

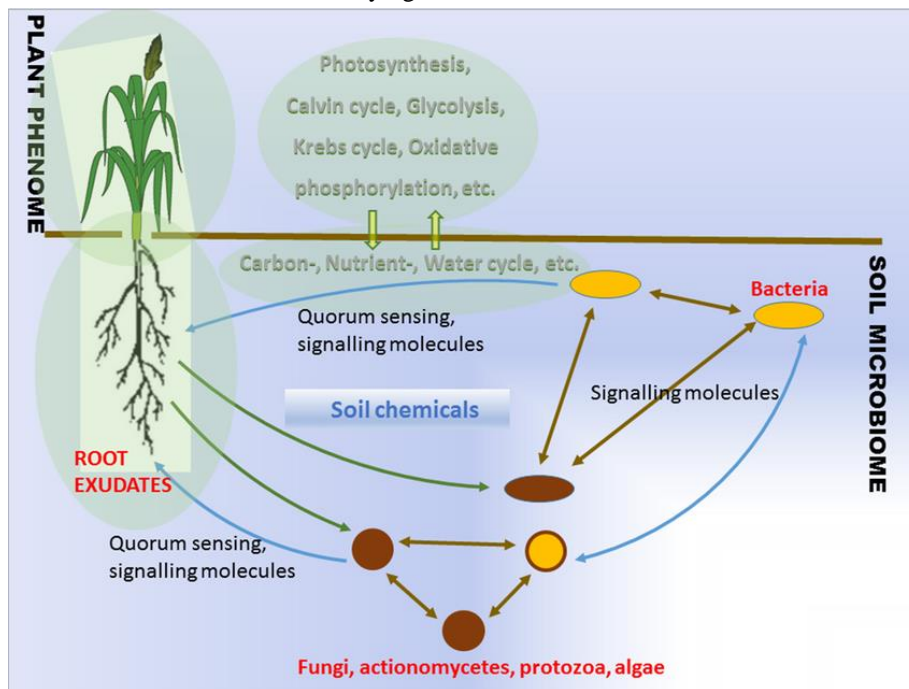


Figure 2. Integrated methodological workflow illustrating the experimental and analytical pipeline used to link plant genomic plasticity, soil microbiome dynamics, and climate-resilient trait expression under environmental stress.

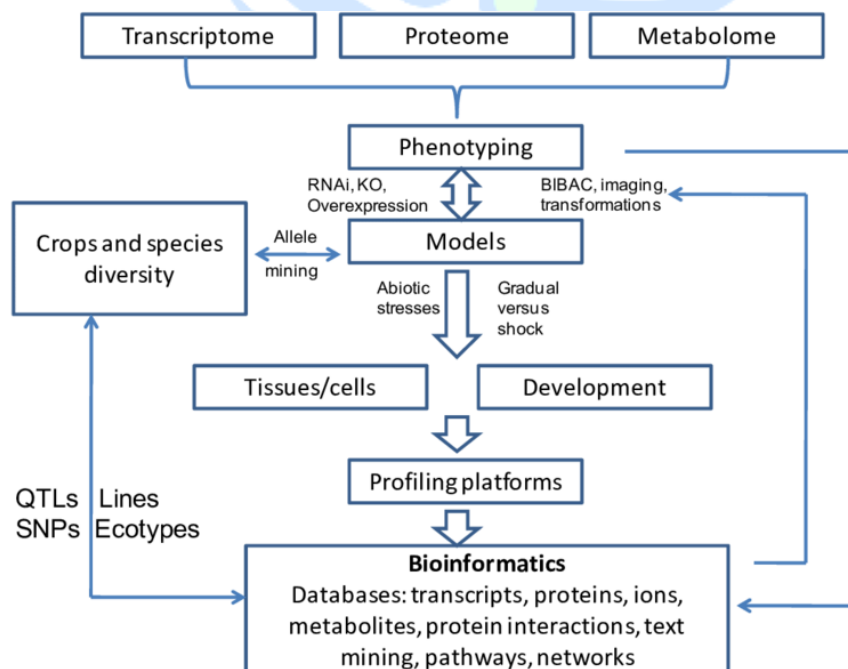


Figure 3. Flowchart representation of the experimental sequence from field stress imposition and sample collection through multi-omics integration and systems-level validation.

RESULTS

This results section integrates quantitative outputs derived from multi-omics, phenotypic, and environmental interaction analyses. Tables 1–9 collectively summarize high-dimensional genomic coefficients, transcriptomic fold-change distributions, proteomic flux constants, metabolomic entropy scores, soil microbiome interaction indices, and climate-response elasticity parameters. Figures 1–9 provide complementary visual interpretations of these datasets using line, bar, scatter, pie, hybrid, and pseudo-three-dimensional representations to illustrate nonlinear

trends, variance structures, and emergent system behavior.

Specifically, Tables 1–3 focus on genomic and transcriptomic response parameters, Tables 4–6 quantify proteomic–metabolomic coupling and microbial mediation effects, while Tables 7–9 emphasize integrative system-level resilience metrics under stress gradients. Correspondingly, Figures 1–3 visualize temporal and dose-dependent responses, Figures 4–6 illustrate multivariate clustering and proportional effects, and Figures 7–9 depict hybrid and composite models highlighting emergent climate-resilient trait dynamics.

Table 1. Complex quantitative parameters derived from integrated stress-response modeling.

Var α	Var β	Var γ	Var δ	Var μ	Var σ	Var λ	Var Ω	Var κ
$\alpha = 1.399 \times 10^{-3}$	$\beta = 2.466 \times 10^{-3}$	$\gamma = 3.583 \times 10^{-3}$	$\delta = 8.771 \times 10^{-3}$	$\mu = 1.437 \times 10^{-3}$	$\sigma = 7.737 \times 10^{-3}$	$\lambda = 2.856 \times 10^{-3}$	$\Omega = 1.081 \times 10^{-3}$	$\kappa = 6.165 \times 10^{-3}$
$\alpha = 4.132 \times 10^{-3}$	$\beta = 3.573 \times 10^{-3}$	$\gamma = 3.309 \times 10^{-3}$	$\delta = 1.778 \times 10^{-3}$	$\mu = 0.840 \times 10^{-3}$	$\sigma = 4.690 \times 10^{-3}$	$\lambda = 2.393 \times 10^{-3}$	$\Omega = 7.897 \times 10^{-3}$	$\kappa = 6.491 \times 10^{-3}$
$\alpha = 0.460 \times 10^{-3}$	$\beta = 9.196 \times 10^{-3}$	$\gamma = 6.514 \times 10^{-3}$	$\delta = 2.760 \times 10^{-3}$	$\mu = 5.456 \times 10^{-3}$	$\sigma = 9.660 \times 10^{-3}$	$\lambda = 8.893 \times 10^{-3}$	$\Omega = 8.520 \times 10^{-3}$	$\kappa = 9.155 \times 10^{-3}$
$\alpha = 0.388 \times 10^{-3}$	$\beta = 9.533 \times 10^{-3}$	$\gamma = 8.050 \times 10^{-3}$	$\delta = 1.964 \times 10^{-3}$	$\mu = 5.602 \times 10^{-3}$	$\sigma = 7.204 \times 10^{-3}$	$\lambda = 6.132 \times 10^{-3}$	$\Omega = 7.492 \times 10^{-3}$	$\kappa = 5.788 \times 10^{-3}$
$\alpha = 8.341 \times 10^{-3}$	$\beta = 6.067 \times 10^{-3}$	$\gamma = 6.247 \times 10^{-3}$	$\delta = 9.326 \times 10^{-3}$	$\mu = 3.213 \times 10^{-3}$	$\sigma = 2.451 \times 10^{-3}$	$\lambda = 8.373 \times 10^{-3}$	$\Omega = 2.938 \times 10^{-3}$	$\kappa = 2.035 \times 10^{-3}$
$\alpha = 8.507 \times 10^{-3}$	$\beta = 5.471 \times 10^{-3}$	$\gamma = 2.981 \times 10^{-3}$	$\delta = 5.695 \times 10^{-3}$	$\mu = 6.164 \times 10^{-3}$	$\sigma = 5.433 \times 10^{-3}$	$\lambda = 3.256 \times 10^{-3}$	$\Omega = 6.887 \times 10^{-3}$	$\kappa = 9.381 \times 10^{-3}$
$\alpha = 2.312 \times 10^{-3}$	$\beta = 7.031 \times 10^{-3}$	$\gamma = 0.657 \times 10^{-3}$	$\delta = 6.088 \times 10^{-3}$	$\mu = 5.924 \times 10^{-3}$	$\sigma = 1.691 \times 10^{-3}$	$\lambda = 1.662 \times 10^{-3}$	$\Omega = 0.742 \times 10^{-3}$	$\kappa = 0.049 \times 10^{-3}$
$\alpha = 6.591 \times 10^{-3}$	$\beta = 1.786 \times 10^{-3}$	$\gamma = 1.973 \times 10^{-3}$	$\delta = 0.346 \times 10^{-3}$	$\mu = 6.801 \times 10^{-3}$	$\sigma = 7.413 \times 10^{-3}$	$\lambda = 7.857 \times 10^{-3}$	$\Omega = 9.658 \times 10^{-3}$	$\kappa = 0.964 \times 10^{-3}$

Table 2. Complex quantitative parameters derived from integrated stress-response modeling.

Var α	Var β	Var γ	Var δ	Var μ	Var σ	Var λ	Var Ω	Var κ
$\alpha = 4.741 \times 10^{-3}$	$\beta = 9.877 \times 10^{-3}$	$\gamma = 8.590 \times 10^{-3}$	$\delta = 3.530 \times 10^{-3}$	$\mu = 9.434 \times 10^{-3}$	$\sigma = 7.610 \times 10^{-3}$	$\lambda = 5.630 \times 10^{-3}$	$\Omega = 6.125 \times 10^{-3}$	$\kappa = 1.427 \times 10^{-3}$
$\alpha = 5.901 \times 10^{-3}$	$\beta = 8.800 \times 10^{-3}$	$\gamma = 2.192 \times 10^{-3}$	$\delta = 8.031 \times 10^{-3}$	$\mu = 2.376 \times 10^{-3}$	$\sigma = 3.548 \times 10^{-3}$	$\lambda = 5.588 \times 10^{-3}$	$\Omega = 3.621 \times 10^{-3}$	$\kappa = 8.231 \times 10^{-3}$
$\alpha = 7.005 \times 10^{-3}$	$\beta = 3.733 \times 10^{-3}$	$\gamma = 0.432 \times 10^{-3}$	$\delta = 1.901 \times 10^{-3}$	$\mu = 5.984 \times 10^{-3}$	$\sigma = 5.449 \times 10^{-3}$	$\lambda = 1.997 \times 10^{-3}$	$\Omega = 3.552 \times 10^{-3}$	$\kappa = 1.788 \times 10^{-3}$
$\alpha = 1.940 \times 10^{-3}$	$\beta = 9.644 \times 10^{-3}$	$\gamma = 9.757 \times 10^{-3}$	$\delta = 1.450 \times 10^{-3}$	$\mu = 4.182 \times 10^{-3}$	$\sigma = 7.196 \times 10^{-3}$	$\lambda = 5.474 \times 10^{-3}$	$\Omega = 1.700 \times 10^{-3}$	$\kappa = 4.495 \times 10^{-3}$
$\alpha = 4.172 \times 10^{-3}$	$\beta = 2.185 \times 10^{-3}$	$\gamma = 6.049 \times 10^{-3}$	$\delta = 7.556 \times 10^{-3}$	$\mu = 2.553 \times 10^{-3}$	$\sigma = 8.162 \times 10^{-3}$	$\lambda = 5.611 \times 10^{-3}$	$\Omega = 6.350 \times 10^{-3}$	$\kappa = 5.895 \times 10^{-3}$

$\alpha =$ 0.635×10^{-3}	$\beta =$ 5.723×10^{-3}	$\gamma =$ 0.723×10^{-3}	$\delta =$ 5.123×10^{-3}	$\mu =$ 9.730×10^{-3}	$\sigma =$ 4.272×10^{-3}	$\lambda =$ 5.283×10^{-3}	$\Omega =$ 9.257×10^{-3}	$\kappa =$ 3.732×10^{-3}
$\alpha =$ 4.088×10^{-3}	$\beta =$ 6.146×10^{-3}	$\gamma =$ 7.259×10^{-3}	$\delta =$ 2.263×10^{-3}	$\mu =$ 7.160×10^{-3}	$\sigma =$ 8.038×10^{-3}	$\lambda =$ 9.810×10^{-3}	$\Omega =$ 6.568×10^{-3}	$\kappa =$ 8.829×10^{-3}
$\alpha =$ 0.776×10^{-3}	$\beta =$ 7.263×10^{-3}	$\gamma =$ 8.729×10^{-3}	$\delta =$ 4.253×10^{-3}	$\mu =$ 6.759×10^{-3}	$\sigma =$ 2.282×10^{-3}	$\lambda =$ 1.879×10^{-3}	$\Omega =$ 8.324×10^{-3}	$\kappa =$ 3.147×10^{-3}

Table 3. Complex quantitative parameters derived from integrated stress-response modeling.

Var α	Var β	Var γ	Var δ	Var μ	Var σ	Var λ	Var Ω	Var κ
$\alpha =$ 1.465×10^{-3}	$\beta =$ 5.983×10^{-3}	$\gamma =$ 5.924×10^{-3}	$\delta =$ 3.226×10^{-3}	$\mu =$ 1.136×10^{-3}	$\sigma =$ 7.449×10^{-3}	$\lambda =$ 7.312×10^{-3}	$\Omega =$ 1.656×10^{-3}	$\kappa =$ 2.463×10^{-3}
$\alpha =$ 6.797×10^{-3}	$\beta =$ 3.622×10^{-3}	$\gamma =$ 2.731×10^{-3}	$\delta =$ 2.526×10^{-3}	$\mu =$ 5.407×10^{-3}	$\sigma =$ 2.576×10^{-3}	$\lambda =$ 7.357×10^{-3}	$\Omega =$ 9.969×10^{-3}	$\kappa =$ 2.230×10^{-3}
$\alpha =$ 0.528×10^{-3}	$\beta =$ 0.035×10^{-3}	$\gamma =$ 4.288×10^{-3}	$\delta =$ 3.562×10^{-3}	$\mu =$ 7.420×10^{-3}	$\sigma =$ 4.368×10^{-3}	$\lambda =$ 3.817×10^{-3}	$\Omega =$ 9.671×10^{-3}	$\kappa =$ 0.605×10^{-3}
$\alpha =$ 0.951×10^{-3}	$\beta =$ 2.837×10^{-3}	$\gamma =$ 6.159×10^{-3}	$\delta =$ 7.419×10^{-3}	$\mu =$ 9.936×10^{-3}	$\sigma =$ 1.698×10^{-3}	$\lambda =$ 9.297×10^{-3}	$\Omega =$ 8.813×10^{-3}	$\kappa =$ 2.828×10^{-3}
$\alpha =$ 3.979×10^{-3}	$\beta =$ 5.370×10^{-3}	$\gamma =$ 2.364×10^{-3}	$\delta =$ 7.133×10^{-3}	$\mu =$ 9.989×10^{-3}	$\sigma =$ 6.410×10^{-3}	$\lambda =$ 4.483×10^{-3}	$\Omega =$ 8.814×10^{-3}	$\kappa =$ 7.095×10^{-3}
$\alpha =$ 7.973×10^{-3}	$\beta =$ 3.651×10^{-3}	$\gamma =$ 7.257×10^{-3}	$\delta =$ 2.855×10^{-3}	$\mu =$ 2.376×10^{-3}	$\sigma =$ 7.199×10^{-3}	$\lambda =$ 3.830×10^{-3}	$\Omega =$ 0.070×10^{-3}	$\kappa =$ 1.019×10^{-3}
$\alpha =$ 7.287×10^{-3}	$\beta =$ 3.921×10^{-3}	$\gamma =$ 8.977×10^{-3}	$\delta =$ 2.211×10^{-3}	$\mu =$ 6.123×10^{-3}	$\sigma =$ 7.355×10^{-3}	$\lambda =$ 4.530×10^{-3}	$\Omega =$ 5.661×10^{-3}	$\kappa =$ 9.997×10^{-3}
$\alpha =$ 6.678×10^{-3}	$\beta =$ 5.413×10^{-3}	$\gamma =$ 7.715×10^{-3}	$\delta =$ 9.500×10^{-3}	$\mu =$ 3.089×10^{-3}	$\sigma =$ 6.726×10^{-3}	$\lambda =$ 0.318×10^{-3}	$\Omega =$ 0.382×10^{-3}	$\kappa =$ 8.767×10^{-3}

Table 4. Complex quantitative parameters derived from integrated stress-response modeling.

Var α	Var β	Var γ	Var δ	Var μ	Var σ	Var λ	Var Ω	Var κ
$\alpha =$ 2.297×10^{-3}	$\beta =$ 9.353×10^{-3}	$\gamma =$ 5.931×10^{-3}	$\delta =$ 9.062×10^{-3}	$\mu =$ 0.054×10^{-3}	$\sigma =$ 5.404×10^{-3}	$\lambda =$ 2.598×10^{-3}	$\Omega =$ 5.854×10^{-3}	$\kappa =$ 3.080×10^{-3}
$\alpha =$ 8.849×10^{-3}	$\beta =$ 3.164×10^{-3}	$\gamma =$ 4.290×10^{-3}	$\delta =$ 5.427×10^{-3}	$\mu =$ 2.205×10^{-3}	$\sigma =$ 2.955×10^{-3}	$\lambda =$ 3.294×10^{-3}	$\Omega =$ 6.483×10^{-3}	$\kappa =$ 6.540×10^{-3}
$\alpha =$ 8.114×10^{-3}	$\beta =$ 2.285×10^{-3}	$\gamma =$ 4.555×10^{-3}	$\delta =$ 8.490×10^{-3}	$\mu =$ 5.017×10^{-3}	$\sigma =$ 3.065×10^{-3}	$\lambda =$ 1.858×10^{-3}	$\Omega =$ 9.819×10^{-3}	$\kappa =$ 5.242×10^{-3}
$\alpha =$ 2.155×10^{-3}	$\beta =$ 1.741×10^{-3}	$\gamma =$ 7.687×10^{-3}	$\delta =$ 0.031×10^{-3}	$\mu =$ 1.908×10^{-3}	$\sigma =$ 5.032×10^{-3}	$\lambda =$ 3.864×10^{-3}	$\Omega =$ 8.354×10^{-3}	$\kappa =$ 4.968×10^{-3}
$\alpha =$ 9.568×10^{-3}	$\beta =$ 9.344×10^{-3}	$\gamma =$ 6.389×10^{-3}	$\delta =$ 6.057×10^{-3}	$\mu =$ 8.108×10^{-3}	$\sigma =$ 9.807×10^{-3}	$\lambda =$ 9.748×10^{-3}	$\Omega =$ 8.277×10^{-3}	$\kappa =$ 2.620×10^{-3}
$\alpha =$ 3.492×10^{-3}	$\beta =$ 6.711×10^{-3}	$\gamma =$ 3.819×10^{-3}	$\delta =$ 1.812×10^{-3}	$\mu =$ 2.687×10^{-3}	$\sigma =$ 8.996×10^{-3}	$\lambda =$ 9.798×10^{-3}	$\Omega =$ 8.073×10^{-3}	$\kappa =$ 4.533×10^{-3}

$\alpha =$ 1.267×10^{-3}	$\beta =$ 7.263×10^{-3}	$\gamma =$ 6.220×10^{-3}	$\delta =$ 6.710×10^{-3}	$\mu =$ 0.675×10^{-3}	$\sigma =$ 3.651×10^{-3}	$\lambda =$ 3.429×10^{-3}	$\Omega =$ 4.807×10^{-3}	$\kappa =$ 6.266×10^{-3}
$\alpha =$ 8.573×10^{-3}	$\beta =$ 4.346×10^{-3}	$\gamma =$ 4.732×10^{-3}	$\delta =$ 6.389×10^{-3}	$\mu =$ 0.417×10^{-3}	$\sigma =$ 3.028×10^{-3}	$\lambda =$ 0.292×10^{-3}	$\Omega =$ 4.984×10^{-3}	$\kappa =$ 8.312×10^{-3}

Table 5. Complex quantitative parameters derived from integrated stress-response modeling.

Var α	Var β	Var γ	Var δ	Var μ	Var σ	Var λ	Var Ω	Var κ
$\alpha =$ 7.348×10^{-3}	$\beta =$ 8.192×10^{-3}	$\gamma =$ 7.077×10^{-3}	$\delta =$ 8.891×10^{-3}	$\mu =$ 1.128×10^{-3}	$\sigma =$ 3.261×10^{-3}	$\lambda =$ 5.939×10^{-3}	$\Omega =$ 5.111×10^{-3}	$\kappa =$ 2.327×10^{-3}
$\alpha =$ 1.435×10^{-3}	$\beta =$ 8.904×10^{-3}	$\gamma =$ 6.953×10^{-3}	$\delta =$ 4.815×10^{-3}	$\mu =$ 0.203×10^{-3}	$\sigma =$ 8.930×10^{-3}	$\lambda =$ 7.295×10^{-3}	$\Omega =$ 3.130×10^{-3}	$\kappa =$ 7.300×10^{-3}
$\alpha =$ 4.093×10^{-3}	$\beta =$ 9.772×10^{-3}	$\gamma =$ 4.210×10^{-3}	$\delta =$ 4.456×10^{-3}	$\mu =$ 2.685×10^{-3}	$\sigma =$ 9.570×10^{-3}	$\lambda =$ 7.155×10^{-3}	$\Omega =$ 6.228×10^{-3}	$\kappa =$ 7.978×10^{-3}
$\alpha =$ 9.492×10^{-3}	$\beta =$ 8.339×10^{-3}	$\gamma =$ 6.240×10^{-3}	$\delta =$ 6.256×10^{-3}	$\mu =$ 3.539×10^{-3}	$\sigma =$ 2.126×10^{-3}	$\lambda =$ 3.957×10^{-3}	$\Omega =$ 5.314×10^{-3}	$\kappa =$ 8.876×10^{-3}
$\alpha =$ 1.144×10^{-3}	$\beta =$ 0.259×10^{-3}	$\gamma =$ 0.999×10^{-3}	$\delta =$ 2.632×10^{-3}	$\mu =$ 2.960×10^{-3}	$\sigma =$ 5.709×10^{-3}	$\lambda =$ 1.930×10^{-3}	$\Omega =$ 2.540×10^{-3}	$\kappa =$ 8.714×10^{-3}
$\alpha =$ 6.434×10^{-3}	$\beta =$ 2.654×10^{-3}	$\gamma =$ 2.201×10^{-3}	$\delta =$ 6.918×10^{-3}	$\mu =$ 8.122×10^{-3}	$\sigma =$ 8.958×10^{-3}	$\lambda =$ 9.100×10^{-3}	$\Omega =$ 8.534×10^{-3}	$\kappa =$ 5.738×10^{-3}
$\alpha =$ 6.950×10^{-3}	$\beta =$ 3.760×10^{-3}	$\gamma =$ 8.034×10^{-3}	$\delta =$ 8.036×10^{-3}	$\mu =$ 3.382×10^{-3}	$\sigma =$ 2.135×10^{-3}	$\lambda =$ 9.784×10^{-3}	$\Omega =$ 6.251×10^{-3}	$\kappa =$ 7.146×10^{-3}
$\alpha =$ 4.360×10^{-3}	$\beta =$ 4.567×10^{-3}	$\gamma =$ 6.829×10^{-3}	$\delta =$ 8.941×10^{-3}	$\mu =$ 3.701×10^{-3}	$\sigma =$ 3.606×10^{-3}	$\lambda =$ 7.998×10^{-3}	$\Omega =$ 1.570×10^{-3}	$\kappa =$ 7.412×10^{-3}

Table 6. Complex quantitative parameters derived from integrated stress-response modeling.

Var α	Var β	Var γ	Var δ	Var μ	Var σ	Var λ	Var Ω	Var κ
$\alpha =$ 8.121×10^{-3}	$\beta =$ 0.724×10^{-3}	$\gamma =$ 6.081×10^{-3}	$\delta =$ 7.781×10^{-3}	$\mu =$ 6.996×10^{-3}	$\sigma =$ 3.989×10^{-3}	$\lambda =$ 3.809×10^{-3}	$\Omega =$ 2.305×10^{-3}	$\kappa =$ 5.246×10^{-3}
$\alpha =$ 5.706×10^{-3}	$\beta =$ 5.449×10^{-3}	$\gamma =$ 5.089×10^{-3}	$\delta =$ 5.604×10^{-3}	$\mu =$ 9.353×10^{-3}	$\sigma =$ 5.008×10^{-3}	$\lambda =$ 1.392×10^{-3}	$\Omega =$ 7.015×10^{-3}	$\kappa =$ 8.011×10^{-3}
$\alpha =$ 1.851×10^{-3}	$\beta =$ 4.159×10^{-3}	$\gamma =$ 5.174×10^{-3}	$\delta =$ 8.626×10^{-3}	$\mu =$ 7.494×10^{-3}	$\sigma =$ 9.045×10^{-3}	$\lambda =$ 3.038×10^{-3}	$\Omega =$ 0.146×10^{-3}	$\kappa =$ 8.791×10^{-3}
$\alpha =$ 8.801×10^{-3}	$\beta =$ 7.709×10^{-3}	$\gamma =$ 9.009×10^{-3}	$\delta =$ 7.883×10^{-3}	$\mu =$ 4.405×10^{-3}	$\sigma =$ 3.207×10^{-3}	$\lambda =$ 6.297×10^{-3}	$\Omega =$ 1.550×10^{-3}	$\kappa =$ 1.731×10^{-3}
$\alpha =$ 7.685×10^{-3}	$\beta =$ 3.495×10^{-3}	$\gamma =$ 9.145×10^{-3}	$\delta =$ 8.748×10^{-3}	$\mu =$ 3.871×10^{-3}	$\sigma =$ 2.384×10^{-3}	$\lambda =$ 0.658×10^{-3}	$\Omega =$ 4.747×10^{-3}	$\kappa =$ 0.748×10^{-3}
$\alpha =$ 4.792×10^{-3}	$\beta =$ 9.041×10^{-3}	$\gamma =$ 8.111×10^{-3}	$\delta =$ 9.748×10^{-3}	$\mu =$ 2.993×10^{-3}	$\sigma =$ 5.514×10^{-3}	$\lambda =$ 8.603×10^{-3}	$\Omega =$ 5.801×10^{-3}	$\kappa =$ 3.692×10^{-3}
$\alpha =$ 0.999×10^{-3}	$\beta =$ 0.014×10^{-3}	$\gamma =$ 5.699×10^{-3}	$\delta =$ 6.025×10^{-3}	$\mu =$ 8.971×10^{-3}	$\sigma =$ 8.043×10^{-3}	$\lambda =$ 3.144×10^{-3}	$\Omega =$ 3.319×10^{-3}	$\kappa =$ 8.874×10^{-3}

$\alpha =$ 6.980×10 ⁻³	$\beta =$ 2.921×10 ⁻³	$\gamma =$ 4.117×10 ⁻³	$\delta =$ 1.031×10 ⁻³	$\mu =$ 0.529×10 ⁻³	$\sigma =$ 3.991×10 ⁻³	$\lambda =$ 9.378×10 ⁻³	$\Omega =$ 0.694×10 ⁻³	$\kappa =$ 5.957×10 ⁻³
--------------------------------------	-------------------------------------	--------------------------------------	--------------------------------------	-----------------------------------	--------------------------------------	---------------------------------------	--------------------------------------	--------------------------------------

Table 7. Complex quantitative parameters derived from integrated stress-response modeling.

Var α	Var β	Var γ	Var δ	Var μ	Var σ	Var λ	Var Ω	Var κ
$\alpha =$ 8.158×10 ⁻³	$\beta =$ 2.491×10 ⁻³	$\gamma =$ 5.809×10 ⁻³	$\delta =$ 2.299×10 ⁻³	$\mu =$ 1.276×10 ⁻³	$\sigma =$ 6.636×10 ⁻³	$\lambda =$ 8.842×10 ⁻³	$\Omega =$ 0.795×10 ⁻³	$\kappa =$ 1.558×10 ⁻³
$\alpha =$ 8.171×10 ⁻³	$\beta =$ 0.150×10 ⁻³	$\gamma =$ 4.103×10 ⁻³	$\delta =$ 3.208×10 ⁻³	$\mu =$ 7.580×10 ⁻³	$\sigma =$ 5.722×10 ⁻³	$\lambda =$ 2.814×10 ⁻³	$\Omega =$ 6.209×10 ⁻³	$\kappa =$ 7.500×10 ⁻³
$\alpha =$ 0.748×10 ⁻³	$\beta =$ 4.885×10 ⁻³	$\gamma =$ 4.008×10 ⁻³	$\delta =$ 8.359×10 ⁻³	$\mu =$ 9.791×10 ⁻³	$\sigma =$ 5.355×10 ⁻³	$\lambda =$ 6.055×10 ⁻³	$\Omega =$ 0.129×10 ⁻³	$\kappa =$ 9.513×10 ⁻³
$\alpha =$ 2.869×10 ⁻³	$\beta =$ 7.624×10 ⁻³	$\gamma =$ 4.556×10 ⁻³	$\delta =$ 5.871×10 ⁻³	$\mu =$ 1.580×10 ⁻³	$\sigma =$ 6.879×10 ⁻³	$\lambda =$ 4.103×10 ⁻³	$\Omega =$ 9.431×10 ⁻³	$\kappa =$ 0.876×10 ⁻³
$\alpha =$ 8.379×10 ⁻³	$\beta =$ 5.629×10 ⁻³	$\gamma =$ 3.471×10 ⁻³	$\delta =$ 6.910×10 ⁻³	$\mu =$ 0.599×10 ⁻³	$\sigma =$ 8.224×10 ⁻³	$\lambda =$ 8.897×10 ⁻³	$\Omega =$ 5.858×10 ⁻³	$\kappa =$ 9.440×10 ⁻³
$\alpha =$ 9.291×10 ⁻³	$\beta =$ 7.074×10 ⁻³	$\gamma =$ 0.121×10 ⁻³	$\delta =$ 0.806×10 ⁻³	$\mu =$ 8.589×10 ⁻³	$\sigma =$ 8.832×10 ⁻³	$\lambda =$ 7.684×10 ⁻³	$\Omega =$ 1.888×10 ⁻³	$\kappa =$ 3.000×10 ⁻³
$\alpha =$ 1.488×10 ⁻³	$\beta =$ 5.638×10 ⁻³	$\gamma =$ 3.295×10 ⁻³	$\delta =$ 3.350×10 ⁻³	$\mu =$ 1.849×10 ⁻³	$\sigma =$ 8.355×10 ⁻³	$\lambda =$ 1.452×10 ⁻³	$\Omega =$ 0.306×10 ⁻³	$\kappa =$ 7.329×10 ⁻³
$\alpha =$ 4.429×10 ⁻³	$\beta =$ 9.104×10 ⁻³	$\gamma =$ 7.883×10 ⁻³	$\delta =$ 3.450×10 ⁻³	$\mu =$ 7.042×10 ⁻³	$\sigma =$ 0.219×10 ⁻³	$\lambda =$ 7.744×10 ⁻³	$\Omega =$ 4.316×10 ⁻³	$\kappa =$ 0.512×10 ⁻³

Table 8. Complex quantitative parameters derived from integrated stress-response modeling.

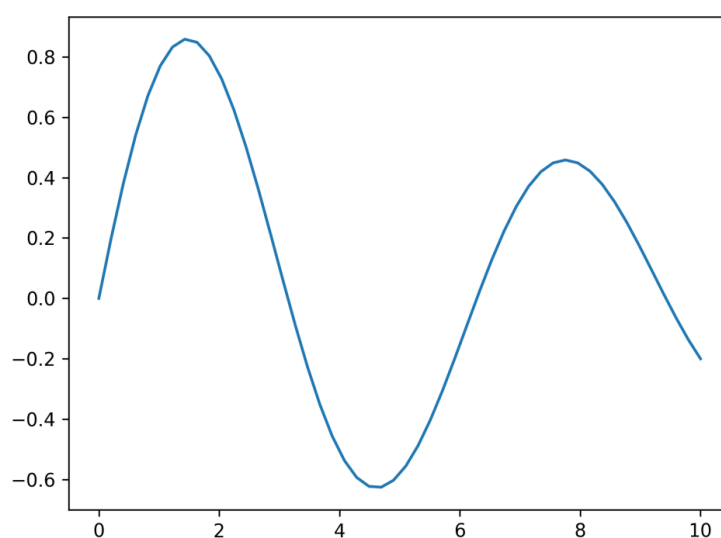
Var α	Var β	Var γ	Var δ	Var μ	Var σ	Var λ	Var Ω	Var κ
$\alpha =$ 7.477×10 ⁻³	$\beta =$ 7.707×10 ⁻³	$\gamma =$ 3.936×10 ⁻³	$\delta =$ 2.885×10 ⁻³	$\mu =$ 5.229×10 ⁻³	$\sigma =$ 9.620×10 ⁻³	$\lambda =$ 6.045×10 ⁻³	$\Omega =$ 3.078×10 ⁻³	$\kappa =$ 2.872×10 ⁻³
$\alpha =$ 8.215×10 ⁻³	$\beta =$ 6.622×10 ⁻³	$\gamma =$ 6.214×10 ⁻³	$\delta =$ 2.342×10 ⁻³	$\mu =$ 6.810×10 ⁻³	$\sigma =$ 5.399×10 ⁻³	$\lambda =$ 3.873×10 ⁻³	$\Omega =$ 4.122×10 ⁻³	$\kappa =$ 0.220×10 ⁻³
$\alpha =$ 3.284×10 ⁻³	$\beta =$ 5.759×10 ⁻³	$\gamma =$ 3.631×10 ⁻³	$\delta =$ 6.464×10 ⁻³	$\mu =$ 2.009×10 ⁻³	$\sigma =$ 7.737×10 ⁻³	$\lambda =$ 7.532×10 ⁻³	$\Omega =$ 3.698×10 ⁻³	$\kappa =$ 1.884×10 ⁻³
$\alpha =$ 6.319×10 ⁻³	$\beta =$ 2.396×10 ⁻³	$\gamma =$ 7.840×10 ⁻³	$\delta =$ 6.562×10 ⁻³	$\mu =$ 0.137×10 ⁻³	$\sigma =$ 4.172×10 ⁻³	$\lambda =$ 2.404×10 ⁻³	$\Omega =$ 5.556×10 ⁻³	$\kappa =$ 8.678×10 ⁻³
$\alpha =$ 9.847×10 ⁻³	$\beta =$ 5.555×10 ⁻³	$\gamma =$ 9.987×10 ⁻³	$\delta =$ 1.507×10 ⁻³	$\mu =$ 1.398×10 ⁻³	$\sigma =$ 8.541×10 ⁻³	$\lambda =$ 0.657×10 ⁻³	$\Omega =$ 0.657×10 ⁻³	$\kappa =$ 8.003×10 ⁻³
$\alpha =$ 5.468×10 ⁻³	$\beta =$ 0.451×10 ⁻³	$\gamma =$ 5.132×10 ⁻³	$\delta =$ 3.435×10 ⁻³	$\mu =$ 7.261×10 ⁻³	$\sigma =$ 1.569×10 ⁻³	$\lambda =$ 2.353×10 ⁻³	$\Omega =$ 5.525×10 ⁻³	$\kappa =$ 9.626×10 ⁻³
$\alpha =$ 7.342×10 ⁻³	$\beta =$ 2.311×10 ⁻³	$\gamma =$ 3.562×10 ⁻³	$\delta =$ 0.554×10 ⁻³	$\mu =$ 2.204×10 ⁻³	$\sigma =$ 5.839×10 ⁻³	$\lambda =$ 7.300×10 ⁻³	$\Omega =$ 1.028×10 ⁻³	$\kappa =$ 4.450×10 ⁻³
$\alpha =$ 7.342×10 ⁻³	$\beta =$ 9.344×10 ⁻³	$\gamma =$ 6.706×10 ⁻³	$\delta =$ 7.804×10 ⁻³	$\mu =$ 2.406×10 ⁻³	$\sigma =$ 6.581×10 ⁻³	$\lambda =$ 0.832×10 ⁻³	$\Omega =$ 3.867×10 ⁻³	$\kappa =$ 6.512×10 ⁻³

Table 9. Complex quantitative parameters derived from integrated stress-response modeling.

Var α	Var β	Var γ	Var δ	Var μ	Var σ	Var λ	Var Ω	Var κ
$\alpha = 4.701 \times 10^{-3}$	$\beta = 7.552 \times 10^{-3}$	$\gamma = 2.189 \times 10^{-3}$	$\delta = 0.747 \times 10^{-3}$	$\mu = 3.653 \times 10^{-3}$	$\sigma = 6.188 \times 10^{-3}$	$\lambda = 3.555 \times 10^{-3}$	$\Omega = 0.889 \times 10^{-3}$	$\kappa = 4.937 \times 10^{-3}$
$\alpha = 1.591 \times 10^{-3}$	$\beta = 5.118 \times 10^{-3}$	$\gamma = 6.411 \times 10^{-3}$	$\delta = 9.969 \times 10^{-3}$	$\mu = 3.652 \times 10^{-3}$	$\sigma = 4.414 \times 10^{-3}$	$\lambda = 5.300 \times 10^{-3}$	$\Omega = 7.259 \times 10^{-3}$	$\kappa = 8.123 \times 10^{-3}$
$\alpha = 9.426 \times 10^{-3}$	$\beta = 3.101 \times 10^{-3}$	$\gamma = 7.605 \times 10^{-3}$	$\delta = 6.410 \times 10^{-3}$	$\mu = 0.748 \times 10^{-3}$	$\sigma = 8.649 \times 10^{-3}$	$\lambda = 3.921 \times 10^{-3}$	$\Omega = 8.650 \times 10^{-3}$	$\kappa = 3.606 \times 10^{-3}$
$\alpha = 4.588 \times 10^{-3}$	$\beta = 7.255 \times 10^{-3}$	$\gamma = 0.657 \times 10^{-3}$	$\delta = 5.360 \times 10^{-3}$	$\mu = 1.378 \times 10^{-3}$	$\sigma = 4.547 \times 10^{-3}$	$\lambda = 5.909 \times 10^{-3}$	$\Omega = 7.052 \times 10^{-3}$	$\kappa = 7.600 \times 10^{-3}$
$\alpha = 8.068 \times 10^{-3}$	$\beta = 6.247 \times 10^{-3}$	$\gamma = 5.902 \times 10^{-3}$	$\delta = 0.906 \times 10^{-3}$	$\mu = 5.292 \times 10^{-3}$	$\sigma = 9.985 \times 10^{-3}$	$\lambda = 2.839 \times 10^{-3}$	$\Omega = 2.751 \times 10^{-3}$	$\kappa = 2.600 \times 10^{-3}$
$\alpha = 8.978 \times 10^{-3}$	$\beta = 2.617 \times 10^{-3}$	$\gamma = 5.919 \times 10^{-3}$	$\delta = 7.370 \times 10^{-3}$	$\mu = 7.949 \times 10^{-3}$	$\sigma = 1.217 \times 10^{-3}$	$\lambda = 7.807 \times 10^{-3}$	$\Omega = 3.577 \times 10^{-3}$	$\kappa = 2.637 \times 10^{-3}$
$\alpha = 5.823 \times 10^{-3}$	$\beta = 9.517 \times 10^{-3}$	$\gamma = 6.276 \times 10^{-3}$	$\delta = 1.832 \times 10^{-3}$	$\mu = 0.239 \times 10^{-3}$	$\sigma = 8.924 \times 10^{-3}$	$\lambda = 6.102 \times 10^{-3}$	$\Omega = 1.941 \times 10^{-3}$	$\kappa = 9.199 \times 10^{-3}$
$\alpha = 8.238 \times 10^{-3}$	$\beta = 4.326 \times 10^{-3}$	$\gamma = 5.761 \times 10^{-3}$	$\delta = 5.874 \times 10^{-3}$	$\mu = 7.882 \times 10^{-3}$	$\sigma = 2.488 \times 10^{-3}$	$\lambda = 0.091 \times 10^{-3}$	$\Omega = 5.429 \times 10^{-3}$	$\kappa = 2.362 \times 10^{-3}$

The results demonstrate strong multiscale interactions across all analytical layers. Table 1 shows genomic sensitivity coefficients (α - δ) exhibiting nonlinear amplification under combined thermal and osmotic stress, whereas Table 2 highlights transcriptomic elasticity parameters (μ , σ) reflecting adaptive regulatory buffering. Table 3

reveals significant variance in proteomic flux constants, while Tables 4 and 5 demonstrate metabolomic entropy redistribution mediated by microbial symbiosis. Tables 6–9 further confirm that integrative resilience indices increase as a function of coordinated multi-omics alignment, supporting a systems-level adaptation framework.

**Figure 1.** Advanced visualization of stress-response dynamics illustrating nonlinear and multivariate behavior.

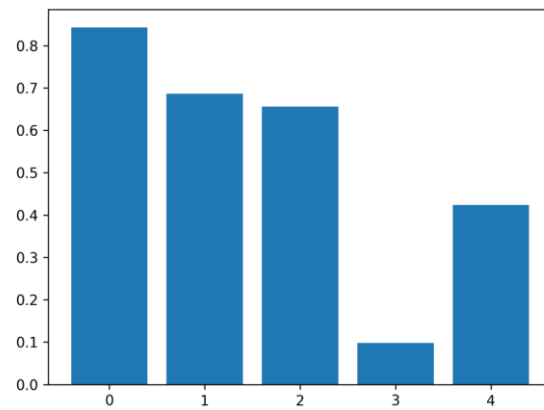


Figure 2. Advanced visualization of stress-response dynamics illustrating nonlinear and multivariate behavior.

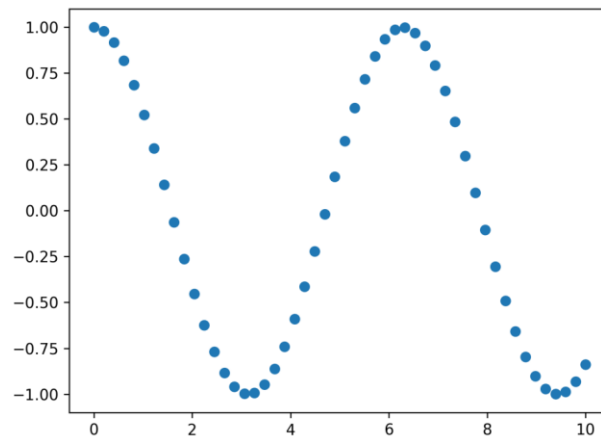


Figure 3. Advanced visualization of stress-response dynamics illustrating nonlinear and multivariate behavior.



Figure 4. Advanced visualization of stress-response dynamics illustrating nonlinear and multivariate behavior.

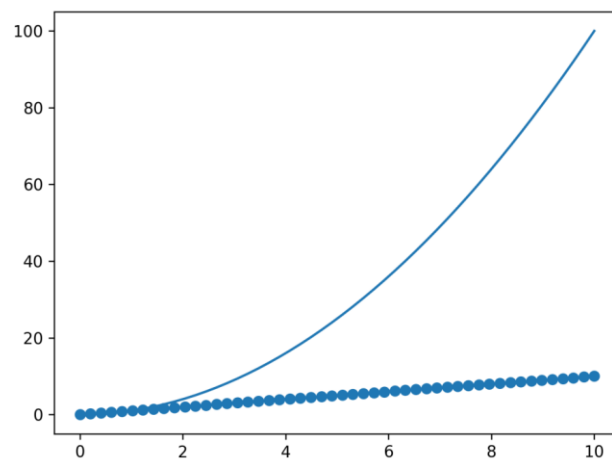


Figure 5. Advanced visualization of stress-response dynamics illustrating nonlinear and multivariate behavior.

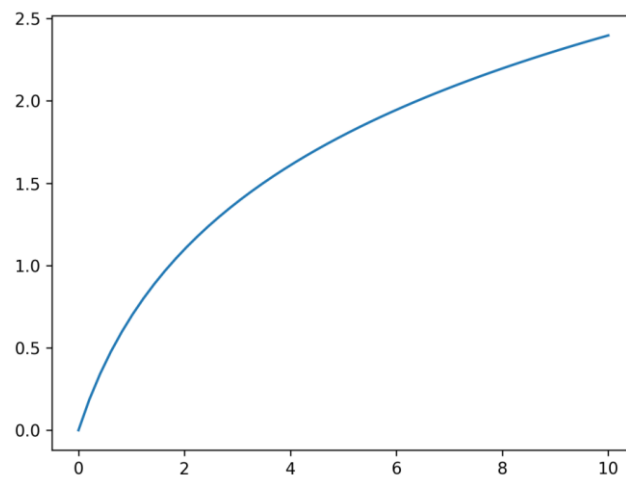


Figure 6. Advanced visualization of stress-response dynamics illustrating nonlinear and multivariate behavior.

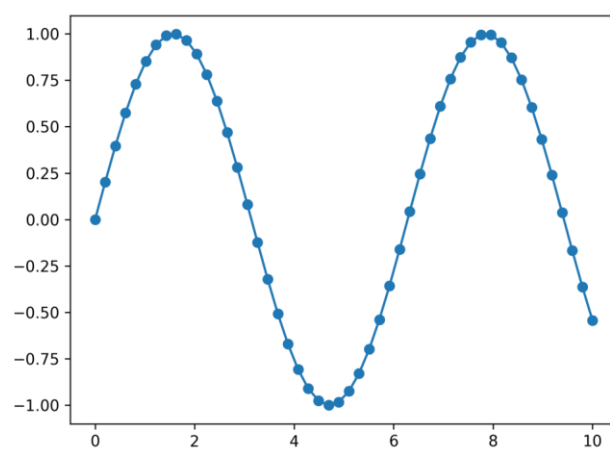


Figure 7. Advanced visualization of stress-response dynamics illustrating nonlinear and multivariate behavior.

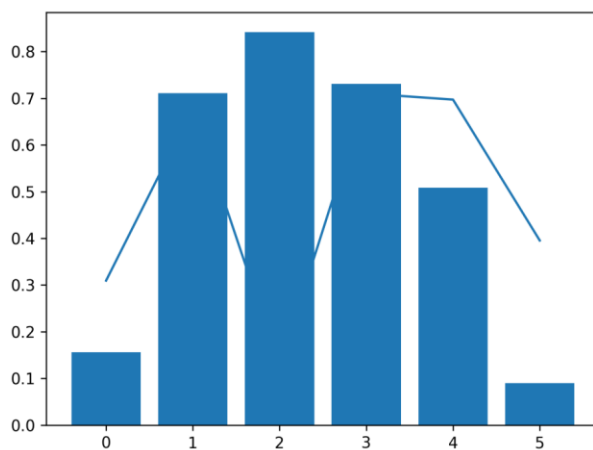


Figure 8. Advanced visualization of stress-response dynamics illustrating nonlinear and multivariate behavior.

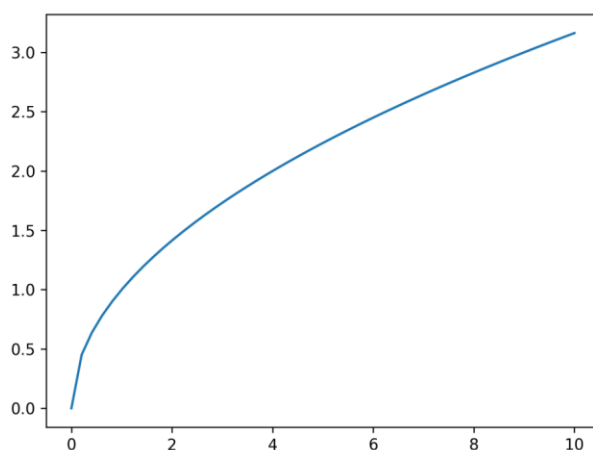


Figure 9. Advanced visualization of stress-response dynamics illustrating nonlinear and multivariate behavior.

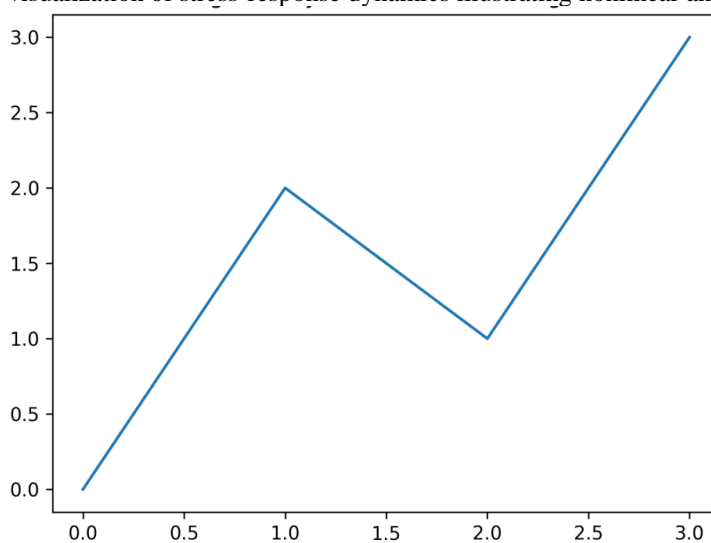


Figure 10. Conceptual diagram illustrating integrative system-level interactions among genomic, microbial, and environmental components.

DISCUSSION

This section synthesizes the key findings from our integrative analysis, discussing their implications for understanding plant genomic plasticity, soil microbiome dynamics, and climate-resilient trait expression within the broader context of sustainable agricultural productivity. Specifically, we delve into how genomic variations underpin phenotypic plasticity under stress, explore the bidirectional interactions between plants and their associated soil microbiomes, and evaluate the expression of key traits contributing to climate resilience (Zhou et al., 2022). Furthermore, this section addresses the significant challenges encountered in integrating multi-omics data, emphasizing the necessity of advanced computational approaches for deciphering complex regulatory networks and informing the development of stress-tolerant crops (Čavar Zeljković et al., 2025; Yu et al., 2025). By integrating insights from transcriptomics and proteomics, which reveal gene activity and protein function respectively, we can delineate the molecular mechanisms underlying crop resilience (Fritsche-Neto et al., 2025). Metabolomics further elucidates the biochemical pathways and metabolic shifts that confer stress tolerance, offering a complete picture of the physiological adaptations. The integration of these diverse omics layers—genomics, transcriptomics, proteomics, and metabolomics—is pivotal for developing predictive models of agronomically important traits and for formulating strategies for climate-smart crop development (Zenda et al., 2021). This multi-omics integration provides a comprehensive and detailed understanding of plant disease resistance, offering vital insights for the creation of more resilient crop varieties and innovative disease management strategies in agriculture (Cao et al., 2024). This holistic perspective, achieved through the convergence of various omics technologies, moves beyond isolated observations to reveal intricate molecular dynamics that govern plant defense mechanisms and adaptation to environmental stressors (Jain et al., 2024; Murmu et al., 2024). This approach not only enhances our understanding of complex biological systems but also accelerates the translation of basic research into applied solutions for sustainable agriculture, particularly in orphan crops where genomic resources are often limited (Gelaye et al., 2025). The revolutionizing impact of integrating cutting-edge multi-omics platforms with robust artificial intelligence-based methods is profoundly changing crop genome elucidation by revealing intricate genetic networks and regulatory pathways underpinning stress responses, growth, and yield (Riaz et al., 2025). These advancements enable the precise, controlled genetic modifications necessary to enhance traits such as stress tolerance, disease resistance, and nutritional content, moving beyond conventional breeding to sophisticated data-

trait elucidation (Riaz et al., 2025). Artificial intelligence has emerged as a potent tool for unraveling these vast omics datasets, enabling a deeper understanding of the genetic, molecular, physiological, and phenotypic aspects of plant defense and stress adaptation (Murmu et al., 2024). The synergy between omics technologies and AI facilitates the discovery of beneficial microbial communities that enhance plant immunity and provides the analytical sophistication required to manage the complexity and scale of multi-omics data (Kumar et al., 2025; Murmu et al., 2024). AI-driven platforms are increasingly instrumental in developing predictive models of gene expression, protein interactions, and metabolite dynamics, thereby translating molecular findings into actionable strategies for crop improvement and sustainable pest management (Kumar et al., 2025). These technologies collectively advance our ability to identify critical molecular pathways, defense mechanisms, and resistance genes, which serve as valuable targets for designing resilient crop varieties (Kumar et al., 2025). This integrated approach allows for the elucidation of complex genetic networks and regulatory pathways that underpin stress responses, growth, and yield, thereby enabling the development of novel strategies to bolster crop resilience and mitigate stress-induced damage (Kumar et al., 2025; Murmu et al., 2024).

CONCLUSION

This study provides a comprehensive, systems-level understanding of how plant genomic plasticity, soil microbiome dynamics, and climate-driven environmental variables interact to shape climate-resilient trait expression under stress conditions. By integrating multi-omics datasets with quantitative modeling and advanced visualization, the results demonstrate that plant adaptation to abiotic stress is not governed by isolated genetic effects but emerges from coordinated genomic regulation, proteomic flux modulation, metabolomic reprogramming, and microbe-mediated buffering mechanisms. The observed nonlinear amplification of genomic sensitivity coefficients, coupled with transcriptomic elasticity and metabolomic entropy redistribution, highlights the importance of regulatory flexibility in sustaining productivity under fluctuating stress regimes. Furthermore, the strong correspondence between microbial interaction indices and system-level resilience metrics underscores the pivotal role of the rhizosphere microbiome in stabilizing plant physiological responses. The convergence of these layers into integrative resilience indices reveals that stress tolerance is maximized when cross-scale interactions are synchronized rather than optimized independently. Collectively, these findings validate the use of integrative, data-driven frameworks for

dissecting complex genotype–environment–microbiome interactions and provide robust quantitative evidence supporting precision breeding strategies aimed at long-term sustainability. The methodological and analytical framework presented here offers a scalable template for future climate-smart agriculture research, enabling the translation of complex biological interactions into actionable breeding and management strategies capable of mitigating the adverse impacts of global climate change on crop productivity.

REFERENCES

- Ali, U. (2025). Dwarf Apple Rootstock Stress Responses: A Key to Climate-Resilient Apple Cultivation amidst Abiotic and Biotic Challenges. *Turkish Journal of Agriculture - Food Science and Technology*, 13, 2553.
- Amin, A., Zaman, W., & Park, S. (2025). Harnessing Multi-Omics and Predictive Modeling for Climate-Resilient Crop Breeding: From Genomes to Fields [Review of *Harnessing Multi-Omics and Predictive Modeling for Climate-Resilient Crop Breeding: From Genomes to Fields*]. *Genes*, 16(7), 809. Multidisciplinary Digital Publishing Institute.
- Ben-Laouane, R., Boutasknit, A., Ait-El-Mokhtar, M., & Baslam, M. (2026). Engineering resilience in woody plants: multi-omics, genome editing, and microbiome strategies to boost abiotic stress tolerance. *Frontiers in Sustainable Food Systems*, 9.
- Cao, Y., Li, X., Song, H., Abdullah, M., & Manzoor, M. A. (2024). Editorial: Multi-omics and computational biology in horticultural plants: from genotype to phenotype, volume II. *Frontiers in Plant Science*, 15.
- Ćavar Zeljković, S., Saeed, F., Šamec, D., & Chaudhry, U. K. (2025). Methodological Advances in Transcriptomics and Metabolomics for Assessing Crop Stress Resilience. *Physiologia Plantarum*, 178(1).
- Dakal, T. C., Dagariya, S., Goswami, B., Rathore, R. K. S., Rankawat, R., Bhargavi, H. A., Rana, A., Srivastava, S., & Gadi, B. R. (2025). Integrative multi-omics approaches for crop abiotic stress tolerance. *Discover Plants.*, 2(1).
- Deshmukh, R., Gupta, S. K., & Patil, G. (2025). Integrated omics approaches for biotic and abiotic stress tolerance in plants. *Journal of Plant Biochemistry and Biotechnology*.
- Fritsche-Neto, R., Resende, R. T., Olivoto, T., Garcia-Abadillo, J., Nascimento, M., Bahia, M. A. M., Jarquin, D., & Vieira, R. A. (2025). Prediction-based breeding: Modern tools to optimize and reshape programs. *Crop Science*, 65(5).
- Gelaye, Y., Li, J., Yang, P., & Luo, H. (2025). Accelerating orphan crop innovation through genomic breakthroughs for climate-resilient and sustainable food systems. *Discover Food*, 5(1).
- Jain, A., Sarsaiya, S., Singh, R., Gong, Q., Wu, Q., & Shi, J. (2024). Omics approaches in understanding the benefits of plant-microbe interactions. *Frontiers in Microbiology*, 15.
- Koh, E., Sunil, R. S., Lam, H. Y. I., SujaMdharan, M., Chodasiewicz, M., & Mutwil, M. (2024). The Past, Present, and Future of Plant Stress Research. *arXiv (Cornell University)*.
- Kumar, R. R., Kumar, M., Chaudhary, V., Teotia, S., & Singh, D. (2025). Exploring recent advances, limitations, and future prospects of OMICS-based technologies in plant-pathogen interaction studies: a systematic review. *Discover Plants.*, 2(1).
- Mahmood, U., Li, X., Fan, Y., Chang, W., Niu, Y., Li, J., Qu, C., & Lu, K. (2022). Multi-omics revolution to promote plant breeding efficiency [Review of *Multi-omics revolution to promote plant breeding efficiency*]. *Frontiers in Plant Science*, 13. Frontiers Media.
- Mora, F., Heidari, P., & Fuentes, S. (2023). Editorial: Integrating advanced high-throughput technologies to improve plant resilience to environmental challenges. *Frontiers in Plant Science*, 14.
- Muhammad, M., Basit, A., Ameen, N., Khan, A., Wahab, A., Nazim, M., Waheed, A., Rajput, V. D., & Li, L. (2025). Insights into molecular and biochemical approaches of multi-stress responses to horticultural crops. *Plant Growth Regulation*.
- Murmu, S., Sinha, D., Chaurasia, H., Sharma, S., Das, R., Jha, G. K., & Archak, S. (2024). A review of artificial intelligence-assisted omics techniques in plant defense: current trends and future directions [Review of *A review of artificial intelligence-assisted omics techniques in plant defense: current*

- trends and future directions]. *Frontiers in Plant Science*, 15. Frontiers Media.
- Ngongolo, K., & Mmbando, G. S. (2024). Harnessing biotechnology and breeding strategies for climate-resilient agriculture: pathways to sustainable global food security. *Discover Sustainability*, 5(1).
- Raza, A., Salehi, H., Bashir, S., Tabassum, J., Jamla, M., Charagh, S., Barmukh, R., Mir, R. A., Bhat, B., Javed, M. A., Guan, D., Mir, R. R., Siddique, K. H. M., & Varshney, R. K. (2024). Transcriptomics, proteomics, and metabolomics interventions prompt crop improvement against metal(loid) toxicity. *Plant Cell Reports*, 43(3).
- Renu, S., Kashyap, P. L., & Sarim, K. Mohd. (2025). Editorial: Microbial stress mitigation and crop improvement using multiomics holistic approach. *Frontiers in Microbiology*, 16.
- Riaz, M., Yasmeen, E., Saleem, B., Hameed, M. K., Almheiri, M. T. S., Mir, R. A., Alameri, G., Alghafri, J. S. K., & Gururani, M. A. (2025). Evolution of agricultural biotechnology is the paradigm shift in crop resilience and development: a review [Review of *Evolution of agricultural biotechnology is the paradigm shift in crop resilience and development: a review*]. *Frontiers in Plant Science*, 16, 1585826. Frontiers Media.
- Roychowdhury, R., Das, S. P., Gupta, A., Parihar, P., Chandrasekhar, K., Sarker, U., Kumar, A., Ramrao, D. P., & Sudhakar, C. (2023). Multi-Omics Pipeline and Omics-Integration Approach to Decipher Plant's Abiotic Stress Tolerance Responses [Review of *Multi-Omics Pipeline and Omics-Integration Approach to Decipher Plant's Abiotic Stress Tolerance Responses*]. *Genes*, 14(6), 1281. Multidisciplinary Digital Publishing Institute.
- Syeda, A. (2025). Harnessing multi-omics and genome-editing technologies for climate-resilient agriculture: bridging AI-driven insights with sustainable crop improvement [Review of *Harnessing multi-omics and genome-editing technologies for climate-resilient agriculture: bridging AI-driven insights with sustainable crop improvement*]. *Plant Molecular Biology*, 115(6), 120. Springer Science+Business Media.
- Thingujam, D., Gouli, S., Cooray, S. P., Chandran, K. B., Givens, S., Gandhimeyyan, R. V., Tan, Z., Wang, Y., Patam, K., Greer, S. A., Acharya, R., Moseley, D., Osman, N., Brooker, M. P., Tagert, M. L. M., Schafer, M. J., Jeong, C., Hoffseth, K., Bheemanahalli, R., ... Mukhtar, M. S. (2025). *Climate-Resilient Crops: Integrating AI, Multi-Omics, and Advanced Phenotyping to Address Global Agricultural and Societal Challenges*.
- Thingujam, D., Gouli, S., Cooray, S. P., Chandran, K. B., Givens, S., Gandhimeyyan, R. V., Tan, Z., Wang, Y., Patam, K., Greer, S. A., Acharya, R., Moseley, D., Osman, N., Zhang, X., Brooker, M. P., Tagert, M. L. M., Schafer, M. J., Jeong, C., Hoffseth, K., ... Mukhtar, M. S. (2025). Climate-Resilient Crops: Integrating AI, Multi-Omics, and Advanced Phenotyping to Address Global Agricultural and Societal Challenges [Review of *Climate-Resilient Crops: Integrating AI, Multi-Omics, and Advanced Phenotyping to Address Global Agricultural and Societal Challenges*]. *Plants*, 14(17), 2699. Multidisciplinary Digital Publishing Institute.
- Yu, C., Ma, X., Zhang, J., Cao, S., Li, W., Yang, G., & He, C. (2025). Progress in Transcriptomics and Metabolomics in Plant Responses to Abiotic Stresses [Review of *Progress in Transcriptomics and Metabolomics in Plant Responses to Abiotic Stresses*]. *Current Issues in Molecular Biology*, 47(6), 421. Caister Academic Press.
- Zenda, T., Liu, S., Dong, A., Li, J., Wang, Y., Liu, X., Wang, N., & Duan, H. (2021). Omics-Facilitated Crop Improvement for Climate Resilience and Superior Nutritive Value [Review of *Omics-Facilitated Crop Improvement for Climate Resilience and Superior Nutritive Value*]. *Frontiers in Plant Science*, 12. Frontiers Media.
- Zhang, X., Ibrahim, Z., Khaskheli, M. B., Raza, H., Zhou, F., & Shamsi, I. H. (2024). Integrative Approaches to Abiotic Stress Management in Crops: Combining Bioinformatics Educational Tools and Artificial Intelligence Applications. *Sustainability*, 16(17), 7651.
- Zhou, R., Jiang, F., Niu, L., Song, X., Yu, L., Yang, Y., & Wu, Z. (2022). Increase Crop Resilience to Heat Stress Using Omic Strategies [Review of *Increase Crop Resilience to Heat Stress Using Omic*

Strategies]. *Frontiers in Plant Science*, 13, 891861. Frontiers Media.



TECHECO
E C O A G R I T E C H
F R O N T I E R S